

## TABLE OF CONTENTS

	<b>Page</b>
<b>ACKNOWLEDGEMENTS</b>	iii
<b>ABSTRACT (ENGLISH)</b>	iv
<b>ABSTRACT (THAI)</b>	vi
<b>LIST OF TABLES</b>	xiv
<b>LIST OF FIGURES</b>	xvii
<b>LIST OF SCHEMES</b>	xxii
<b>ABBREVIATIONS</b>	xxiii
<b>CHAPTER 1 INTRODUCTION</b>	
1.1 Biodegradable Polymers	1
1.2 Biodegradable Polymers for Use in Biomedical Applications	2
1.2.1 Surgical Sutures	2
1.2.2 Tissue Repair and Regeneration	4
1.2.3 Drug Delivery Systems	7
1.3 Ring-Opening Polymerization of Cyclic Esters	8
1.3.1 Homopolymers	9
1.3.1.1 Polylactide, PL	10
1.3.1.2 Poly( $\epsilon$ -caprolactone), PCL	11
1.3.2 Coordination-Insertion Ring-Opening Polymerization	12
1.3.3 Transesterification Reactions	13
1.3.4 Initiators/Catalysts for the Ring-Opening Polymerization	14

ลิขสิทธิ์มหาวิทยาลัยเชียงใหม่  
Copyright © by Chiang Mai University  
All rights reserved

	<b>Page</b>	
1.4	Controlled Molecular Architecture	17
1.5	Degradation Phenomena in Biodegradable Polymers	20
1.6	<i>In Vitro</i> Hydrolytic Degradation Testing	22
1.6.1	Weight Loss	22
1.6.2	Polymer Morphology	23
1.6.3	pH	23
1.7	Previous Work Relevant to This Study	24
1.8	Aims of This Study	27
<b>CHAPTER 2 EXPERIMENTAL METHODS</b>		
2.1	Chemicals, Apparatus and Instruments	30
2.1.1	Chemicals	30
2.1.2	Apparatus and Instruments	31
2.2	Monomer Preparation and Purification	33
2.2.1	Synthesis of L-Lactide	33
2.2.2	Purification and Purity Analysis of L-Lactide	35
2.2.3	Purification of $\epsilon$ -Caprolactone by Vacuum Distillation	36
2.3	Catalyst and Initiator Purification	37
2.3.1	Stannous Octoate	37
2.3.2	1-Hexanol	38
2.3.3	Pentaerythritol	38
2.4	Characterization Methods	38
2.4.1	Fourier Transform Infrared Spectroscopy (FT-IR)	38

	<b>Page</b>
2.4.2 High Resolution Mass Spectroscopy (HR-MS)	39
2.4.3 Nuclear Magnetic Resonance Spectroscopy (NMR)	39
2.4.4 Gel Permeation Chromatography (GPC)	40
2.4.5 Differential Scanning Calorimetry (DSC)	40
2.4.6 Thermogravimetric Analysis (TGA)	41
2.4.7 Dilute-Solution Viscometry	41
2.4.8 Mechanical Tensile Testing	41
2.4.9 Melt Rheology Measurements	42
2.5 Synthesis of Pentaerythritol tetrakis(6'-hydroxyhexanoate) Star-Core Macroinitiator	43
2.5.1 Synthesis of Methyl 6-hydroxyhexanoate ( <b>2</b> )	43
2.5.2 Synthesis of Methyl 6-(tetrahydro-2 <i>H</i> -pyran-2-yloxy)hexanoate ( <b>3</b> )	46
2.5.3 Synthesis of 6-(Tetrahydro-2 <i>H</i> -pyran-2-yloxy)hexanoic acid ( <b>4</b> )	48
2.5.4 Synthesis of Pentaerythritol tetrakis(6'-hydroxyhexanoate) ( <b>7</b> )	51
2.6 Polymer Synthesis and Purification	54
2.6.1 Synthesis of Low Molecular Weight Poly( $\epsilon$ -caprolactone), PCL Model Compounds with Different Molecular Architectures	55
2.6.2 Synthesis of High Molecular Weight Poly( $\epsilon$ -caprolactone), PCL with Different Molecular Architectures	56

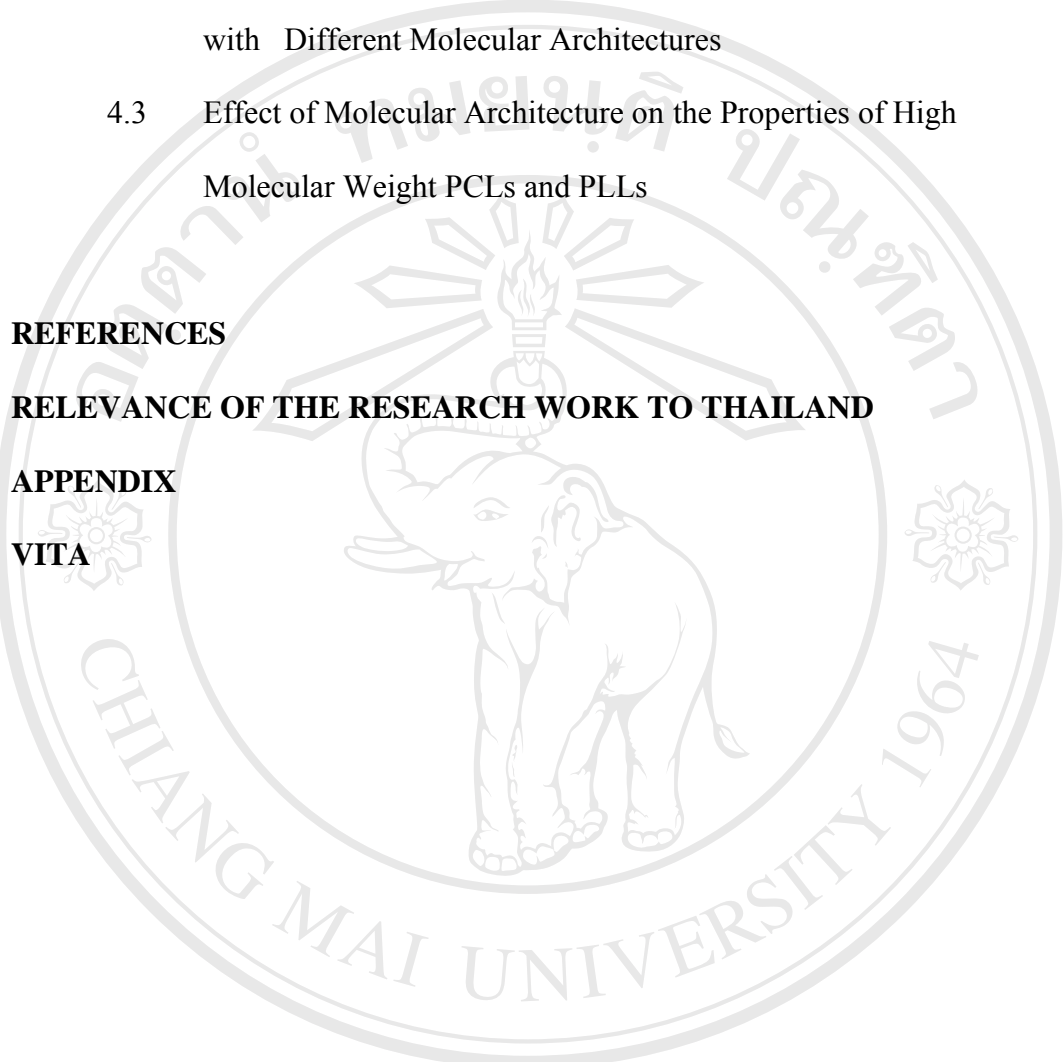
	<b>Page</b>
2.6.3 Synthesis of High Molecular Weight Poly(L-lactide), PLL with Different Molecular Architectures	57
2.7 <i>In Vitro</i> Hydrolytic Biodegradation Studies	58
2.7.1 Preparation of Phosphate Buffer Saline (PBS)	59
2.7.2 Preparation of Polymer Samples and Glassware	59
2.7.3 Sampling Procedure	61
 <b>CHAPTER 3 RESULTS AND DISCUSSION</b>	
3.1 Synthesis of Pentaerythritol tetrakis(6'-hydroxyhexanoate)	62
3.2 Synthesis of Low Molecular Weight PCL Model Compounds with Different Molecular Architectures	69
3.2.1 Molecular Weight Determination of PCL Model Compounds by GPC and Dilute-Solution Viscometry	72
3.2.2 Structural Analysis and Molecular Weight Determination of PCL Model Compounds by <sup>1</sup> H-NMR Spectroscopy	79
3.2.3 Thermal Characterization of PCL Model Compounds by DSC	84
3.2.4 Thermal Characterization of PCL Model Compounds by TGA	86
3.3 Synthesis and Characterization of High Molecular Weight PCL with Different Molecular Architectures	88
3.3.1 Molecular Weight Determinations of High Molecular Weight PCL by GPC and Dilute-Solution Viscometry	90

	<b>Page</b>
3.3.2 Thermal Characterization of High Molecular Weight PCL by DSC	91
3.3.3 Thermal Characterization of High Molecular Weight PC by TG	93
3.3.4 Mechanical Properties of High Molecular Weight PCL by Tensile Testing	94
3.3.5 Rheological Properties of High Molecular Weight by Melt Rheology Measurement	95
3.4 Synthesis and Characterization of High Molecular Weight PLL with Different Molecular Architectures	96
3.4.1 Molecular Weight Determinations of High Molecular Weight PLL by Dilute-Solution Viscometry	97
3.4.2 Thermal Characterization of High Molecular Weight PLL by DSC	100
3.5 <i>In Vitro</i> Hydrolytic Biodegradation Studies of High Molecular Weight PCL and PLL	102
3.5.1 Weight Loss Profiles	104
3.5.2 pH Stability of Phosphate Immersion Medium	111
3.5.3 Morphology Determination by DSC	113

## CHAPTER 4 CONCLUSIONS

4.1 Synthesis of Pentaerythritol tetrakis(6'-hydroxyhexanoate) Star- Core Macroinitiator	121
---	-----

	<b>Page</b>
4.2 Synthesis of Low Molecular Weight PCLs Model Compounds with Different Molecular Architectures	122
4.3 Effect of Molecular Architecture on the Properties of High Molecular Weight PCLs and PLLs	124
<b>REFERENCES</b>	128
<b>RELEVANCE OF THE RESEARCH WORK TO THAILAND</b>	134
<b>APPENDIX</b>	135
<b>VITA</b>	156



ลิขสิทธิ์มหาวิทยาลัยเชียงใหม่

Copyright© by Chiang Mai University

All rights reserved

## LIST OF TABLES

<b>Table</b>	<b>Page</b>
2.1 Chemicals used in this research project.	30
2.2 Apparatus and instruments used in this research project.	32
2.3 Data of compound 2.	45
2.4 Data of compound 3.	47
2.5 Data of compound 4.	49
2.6 Data of compound 7.	53
2.7 Polymerization conditions of low molecular weight PCLs with different molecular architectures synthesis at 120°C for 48 hours.	56
2.8 Polymerization conditions for high molecular weight PCLs with different molecular architectures synthesis at 120°C for 72 hours (10 g).	56
2.9 Polymerization conditions for high molecular weight PCLs with different molecular architectures synthesis at 120°C for 72 hours (25 g).	57
2.10 Polymerization conditions for low molecular weight PLLs with different molecular architectures synthesis at 120°C for 48 hours (10 g).	58
2.11 Polymerization conditions for high molecular weight PLLs with different molecular architectures synthesis at 120°C for 72 hours (25 g).	58
3.1 The results of low molecular weight PCL model compound with different molecular architectures.	70
3.2 Dilute-solution viscometry data of low molecular weight PCL_macroinitiator using THF as solvent at 30°C.	76

	<b>Page</b>
3.3 Proton assignments and corresponding chemical shift ranges for the various resonance peaks in the <sup>1</sup> H-NMR spectra of the linear and star-shaped low molecular weight purified PCL model compounds.	81
3.4 Proton assignments and corresponding peak area integrations for the various resonance peaks in the <sup>1</sup> H-NMR spectra of the linear and star-shaped low molecular weight purified PCLs model compounds.	81
3.5 The results of high molecular weight PCL with different molecular architectures.	88
3.6 The results of high molecular weight PLL homopolymer with different molecular architectures.	99
3.7 The results of the high molecular weight PCLs with different molecular architectures use for <i>in vitro</i> hydrolytic degradation study.	103
3.8 The results of the high molecular weight PLLs with different molecular architectures use for <i>in vitro</i> hydrolytic degradation study.	104
3.9 Weight, % weight loss, % weight retention and pH of homopolymer PCL_1-hexanol immersed in PBS medium at 37±1.0°C.	105
3.10 Weight, % weight loss, % weight retention and pH of homopolymer PCL_PTOL immersed in PBS medium at 37±1.0°C.	106
3.11 Weight, % weight loss, % weight retention and pH of homopolymer PCL_macroinitiator immersed in PBS medium at 37±1.0°C.	106
3.12 Weight, % weight loss, % weight retention and pH of homopolymer PLL_1-hexanol immersed in PBS medium at 37±1.0°C.	107
3.13 Weight, % weight loss, % weight retention and pH of homopolymer PLL_PTOL immersed in PBS medium at 37±1.0°C.	107



	<b>Page</b>
3.14 Weight, % weight loss, % weight retention and pH of homopolymer PLL_macroinitiator immersed in PBS medium at $37\pm 1.0^{\circ}\text{C}$ .	108
3.15 DSC results for first run of linear PLL_1-hexanol immersed in PBS medium at $37\pm 1.0^{\circ}\text{C}$ .	114
3.16 DSC results for second run of linear PLL_1-hexanol immersed in PBS medium at $37\pm 1.0^{\circ}\text{C}$ .	115
3.17 DSC results for first run of star-shaped PLL_PTOL immersed in PBS medium at $37\pm 1.0^{\circ}\text{C}$ .	115
3.18 DSC results for second run of star-shaped PLL_PTOL immersed in PBS medium at $37\pm 1.0^{\circ}\text{C}$ .	116
3.19 DSC results for first run of star-shaped PLL_macroinitiator immersed in PBS medium at $37\pm 1.0^{\circ}\text{C}$ .	116
3.20 DSC results for second run of star-shaped PLL_macroinitiator immersed in PBS medium at $37\pm 1.0^{\circ}\text{C}$ .	117

## LIST OF FIGURES

Figure	Page
1.1 Biodegradable monofilament sutures: commercial product (a) Dexon <sup>®</sup> and (b) Maxon <sup>®</sup> . [5, 6]	4
1.2 Synthetic biodegradable monofilament suture, poly(lactide- <i>co</i> - $\epsilon$ -caprolactone- <i>co</i> -glycolide), poly(LL- <i>co</i> -CL- <i>co</i> -G) prototype, from Biomedical Polymers Technology Unit. [10]	4
1.3 Nerve repair methods (a) nerve suture (b) nerve graft and (c) nerve guide.	6
1.4 Synthetic biodegradable nerve guide tubes of (a) poly(DL- <i>co</i> -CL) from Neurolac <sup>®</sup> [13] (b) poly(LL- <i>co</i> -CL- <i>co</i> -G) from Biomedical Polymers Technology Unit. [15]	7
1.5 Equation representing the ROP of a cyclic ester. (R = (CH <sub>2</sub> ) <sub>0-3</sub> and/or CHR", M = metal).	9
1.6 Structures of the different stereoforms of the lactide monomer and the resulting polymer repeating unit, with the chiral center marked with *. (a) L-lactide (LL), (b) D-lactide (DL) and (c) <i>meso</i> -lactide.	10
1.7 The reaction pathway for the ROP of a cyclic ester by the coordination-insertion mechanism.	13
1.8 Reaction schemes for transesterification reaction; (a) intermolecular transesterification and (b) intramolecular transesterification (back-biting).	14
1.9 Tin (II) 2-ethylhexanoate or stannous octoate (SnOct <sub>2</sub> ).	15

	<b>Page</b>
1.10 The main ROP mechanism proposals with SnOct <sub>2</sub> as catalyst that the complexation of a monomer and alcohol prior to ROP.	16
1.11 The main ROP mechanism proposals with SnOct <sub>2</sub> as catalyst that the formation of a tin alkoxide before ROP of cyclic ester.	16
1.12 Illustrations of the three approaches for the synthesis of a star-branched polymer (a) the core-first method (b) and (c) the arm-first method. [33]	18
1.13 Representation of structures of polymers with different molecular architectures: (a) linear, (b) branch, (c) star-branch and (d) network.	19
1.14 Simple hydrolysis of aliphatic polyester.	21
2.1 Two-step process used for synthesizing LL from L(+)-lactic acid.	33
2.2 The apparatus used in the synthesis of LL. [61]	34
2.3 DSC melting peak of synthesized LL (after 3 <sup>rd</sup> recrystallisation) (sample size = 2.850 mg, heating rate = 2°C/min).	36
2.4 Vacuum distillation apparatus used for the purification of ε-caprolactone.	37
2.5 Bohlin Gemini HR <sup>nano</sup> Rotational Rheometer apparatus; (a) parallel plate geometry and (b) the gap between the plates.	43
2.6 Apparatus used in (a) the ring-opening bulk polymerization and (b) polymer purification by re-precipitation from solution.	55
2.7 Incubator for <i>in vitro</i> hydrolytic degradation studies.	60
3.1 <sup>1</sup> H-NMR spectra data of compound <b>2</b> .	63
3.2 <sup>1</sup> H-NMR spectra data of compound <b>3</b> .	64
3.3 <sup>1</sup> H-NMR spectra data of compound <b>4</b> .	65

	<b>Page</b>
3.4	<sup>1</sup> H-NMR spectra data of compound 7. 67
3.5	IR data of compound 7. 67
3.6	Polymerization of $\epsilon$ -caprolactone using 0.1 mole % SnOct <sub>2</sub> as a catalyst and 4 mole% of (a) 1-hexanol (b) PTOL and (c) pentaerythritol tetrakis (6'-hydroxyhexanoate) as initiators at 120°C for 48 hours. 69
3.7	GPC curves of low molecular weight purified PCL model compounds; (a) PCL_1-hexanol (b) PCL_PTOL and (c) PCL_macroinitiator. 73
3.8	Reduced ( $\eta_{red}$ ) and inherent ( $\eta_{inh}$ ) viscosity-concentration plots of low molecular weight; (a) PCL_1-hexanol, (b) PCL_PTOL and (c) PCL_macroinitiator (◆ $\eta_{red}$ and ■ $\eta_{inh}$ ). 76
3.9	<sup>1</sup> H-NMR spectrum of low molecular weight crude PCLs; (a) PCL_1-hexanol (b) PCL-PTOL and (c) PCL-macroinitiator recorded in CDCl <sub>3</sub> . 80
3.10	Comparison of the DSC thermograms first run of linear and star-shaped low molecular weight PCLs model compounds. 84
3.11	Comparison of the DSC thermograms second run of linear and star-shaped low molecular weight PCLs model compounds. 84
3.12	Comparison of the TG thermograms of PCL model compounds; (a) PCL_1-hexanol, (b) PCL_PTOL and (C) PCL_macroinitiator. 86
3.13	Comparison of the DSC thermograms first run of linear and star-shaped high molecular weight poly( $\epsilon$ -caprolactone) homopolymers. 91
3.14	Comparison of the DSC thermograms second run of linear and star-shaped high molecular weight poly( $\epsilon$ -caprolactone) homopolymers. 91

	<b>Page</b>
3.15 Comparison of the TG thermograms of homopolymers; (a) PCL_1-Hexanol, (b) PCL_PTOL and (C) PCL_macroinitiator.	91
3.16 Comparison of the stress-strain curve of homopolymer; (a) PCL_1- Hexanol, (b) PCL_PTOL and (C) PCL_macroinitiator.	93
3.17 The viscosity and stress vs. shear rate (1/s) of linear and star-shaped PCL at 80°C.	95
3.18 Polymerization of L-lactide using (a) 1-hexanol (b) PTOL and (c) pentaerythritol tetrakis(6'-hydroxyhexanoate) as initiators.	98
3.19 Comparison of the DSC thermograms 1 <sup>st</sup> run of the linear and star- shaped PLLs homopolymer.	101
3.20 Comparison of the DSC thermograms 2 <sup>nd</sup> run of the linear and star- shaped PLLs homopolymer.	102
3.21 Comparison of % weight retention of linear and star-shape PLL during of the period of the in vitro biodegradation experiments.	109
3.22 Comparison of the DSC thermograms 1 <sup>st</sup> run of the linear and star- shaped PLLs homopolymer.	109
3.23 Comparison of the DSC thermograms 2 <sup>nd</sup> run of the linear and star- shaped PLLs homopolymer.	112
3.24 Comparison of the DSC thermograms first heating run of PLL_1-hexanol during of the period of the in vitro biodegradation experiments.	117
3.25 Comparison of the DSC thermograms first heating run of PLL_PTOL during of the period of the <i>in vitro</i> biodegradation experiments.	118

	<b>Page</b>
3.26 Comparison of the DSC thermograms first heating run PLL_macroinitiator during of the period of the <i>in vitro</i> biodegradation experiments.	118
3.27 Comparison of the DSC thermograms second run of PLL_1-hexanol during of the period of the <i>in vitro</i> biodegradation experiments.	119
3.28 Comparison of the DSC thermograms second heating run of PLL_PTOL during of the period of the <i>in vitro</i> biodegradation experiments.	119
3.29 Comparison of the DSC thermograms second heating run PLL_macroinitiator during of the period of the <i>in vitro</i> biodegradation experiments.	120

**LIST OF SCHEMES**

<b>SCHEME</b>	<b>Page</b>
3.1 Retrosynthesis of pentaerythritol tetrakis(6'-hydroxyhexanoate)	61
3.2 Synthesis of pentaerythritol tetrakis(6'-hydroxyhexanoate) (7)	62
3.3 Translation of methyl 6-hydroxyhexanoate (2)	62
3.4 Protection of alcohol by using DHP and M-K10	63
3.5 Hydrolysis of compound 3	64
3.6 Esterification and deprotection of compound 7	66

## ABBREVIATIONS

LL	L-lactide
DL	D-lactide
DLL	D,L-lactide
CL	$\epsilon$ -caprolactone
G	glycolide
PL	polylactide
PCL	poly( $\epsilon$ -caprolactone)
PG	polyglycolide
FDA	Food and Drug Administration
ROP	ring-opening polymerization
SnOct <sub>2</sub>	stannous octoate
Sn( <i>On</i> Bu) <sub>2</sub>	tin(II) <i>n</i> -butoxide
CDCl <sub>3</sub>	deuterated chloroform
THF	tetrahydrofuran
PTOL	pentaerythritol
TMP	1,1,1-tris(hydroxymethyl)propane
DPTOL	dipentaerythritol
DHP	3,4-dihydro-2 <i>H</i> -pyran
DCC	<i>N,N'</i> -dicyclohexylcarbodiimide
DMAP	4-dimethylaminopyridine
DMF	<i>N,N</i> -dimethylformamide



PBS	phosphate buffer saline
Na <sub>2</sub> HPO <sub>4</sub>	disodium hydrogen orthophosphate
NaCl	sodium chloride
NaOH	sodium hydroxide
FT-IR	fourier transform infrared spectroscopy
<sup>1</sup> H-NMR	proton nuclear magnetic resonance
<sup>13</sup> C-NMR	carbon-13 nuclear magnetic resonance
HR-MS	high resolution mass spectroscopy
DSC	differential scanning calorimetry
TG	thermogravimetry
GPC	gel permeation chromatography
$\bar{M}_n$	number-average molecular weight
$\bar{M}_w$	weight-average molecular weight
$\bar{M}_v$	viscosity-average molecular weight
$\bar{M}_w / \bar{M}_n$ , MWD	molecular weight distribution
T <sub>g</sub>	glass transition temperature
T <sub>c</sub>	crystallization temperature
T <sub>m</sub>	melting temperature
T <sub>d</sub>	decomposition temperature
$\eta$	intrinsic viscosity
$\eta_0$	zero shear rate viscosity
h	hour
g	gram

cm	centimeter
mm	millimeter
ml	milliliter
g dl <sup>-1</sup>	grams per deciliter
g mole <sup>-1</sup>	grams per mole
mmHg	millimeters of mercury
MHz	megahertz
MPa	megapascal
Pa	pascal
°C	degree Celsius
°C min <sup>-1</sup>	degree Celsius per minutes
rpm	round per minute
cm <sup>-1</sup>	wavenumber
calc.	calculated
conc.	concentration
s	singlet (spectral)
t	triplet (spectral)
m	multiplet (spectral)
dt	double of triplet (spectral)
ppm	parts per million (in NMR)
δ	chemical shift (ppm)
eq.	equivalent

ลิขสิทธิ์มหาวิทยาลัยเชียงใหม่

Copyright © by Chiang Mai University

All rights reserved